

Impact of WBG-Semiconductors on Automotive Communication Networks

Carina Austermann, Stephan Frei
On-board Systems Lab
TU Dortmund University
Dortmund, Germany
carina.austermann@tu-dortmund.de

Abstract—Electromagnetic disturbances from power electronic systems can affect communication networks, especially in the automotive wiring harness with its limited distance between wires. The introduction of Wide-Band-Gap (WBG) semiconductors in power electronic systems enables smaller components and higher efficiency due to higher frequencies and steeper slopes of the PWM control signals. Furthermore, the increasing energy demands lead to a raise of the voltage level up to 48 V. In contrast to high voltage automotive systems with complex shielded cables for EV (Electric Vehicles), unshielded cables are applied in 48 V cabling systems. The use of fast switching power electronic devices in combination with the increased voltage level pose a new challenge on electromagnetic compatibility in automotive environment. This paper shows investigations on the immunity of communication networks under these new conditions. Therefore, measurement and simulative analysis are presented to estimate the potential impact on the reliability of data transmission.

Keywords—PWM, power electronics, WBG, EMI, cable coupling, LIN, CAN

I. INTRODUCTION

Due to increasing energy demands, the voltage level in automobiles has been raised up to 48 V. In contrast to high voltage automotive systems for electric propulsion systems, simple cables without shield are applied. Besides, with the introduction of transistors based on WBG-semiconductors power electronics with increased efficiency can be implemented [1]. High frequency switching operation of power electronics devices due to pulse width modulation (PWM) generates common and differential mode disturbing signals on adjacent wires in the wiring harness by near-field coupling. The generated distributions caused by the use of WBG semiconductors are investigated in some publications (e.g. [2], [3]). In [3] the impact of PWM signals generated by a motor drive system on power line communication is analyzed. It can be seen, that output signals of power electronics lead to a wide spectrum of the interference voltages with an impact on the communication signals. In contrast to [3] this paper focusses on direct cable coupling to common automotive bus systems. As unshielded cables are state of the art today, the investigations are limited to such cables.

In this paper, investigations on the impact of higher switching frequencies and a higher voltage level on communication performance are presented. The crosstalk coupling configuration is shown in Fig. 1. A control device with GaN transistor and a resistive load build up a simple power elec-

tronic system for e.g. electromagnetic valve control. The control device generates rectangular voltage pulses as PWM control signal. The simplified communication network consists of a point-to-point connection of two nodes. The nodes and the cable type depend on the implemented bus system. In the following investigations, LIN and CAN Bus systems are used as common communication standards in automotive environments. Therefore, the nodes are connected with a single wire (LIN) or unshielded twisted wire pair (CAN) as depicted in Fig. 1.

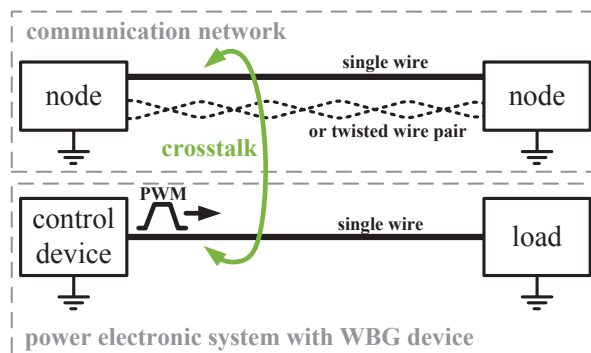


Fig. 1. Investigated setup

The purpose of this paper is to show the behavior of commonly used bus systems under the impact of 48 V and steep rise times. In section II the WBG semiconductor technology and its advantages are described. Therefore, section III summarizes common automotive communication networks, which will be analyzed in this paper. The modeling approaches for the simulation investigations are introduced in Section IV and validated in V with measurement results. Finally, section VI concludes this paper.

II. POWER ELECTRONIC SYSTEMS

Power electronics is a developing sector with many automotive applications, e.g. DC/DC-converters, motor drive applications, power distribution units [4]. There were many investigations on power MOSFETs and IGBTs, which have been improved close to their theoretical limits [1]. However, the switching frequency is limited to some hundreds of kilohertz by its gate drive loss [1]. The utilization of WBG semiconductors allows applications with operation frequencies up to the megahertz range combined with good thermal properties. Higher voltage ranges to face the increasing power demand accompany the electrification in automobiles. The WBG semiconductors are also suitable to be used with higher voltage ranges. The most promising WBG semiconductors for power electronics up today are Gallium nitride (GaN) and Silicon carbide (SiC). This better performance is based on their material properties such as a high electron mobility, high breakdown field, and high electron velocity, as in table 1.

WBG-based power electronics feature both low on-resistance in conduction and low switching losses [1]. GaN transistors achieved switching speeds up to 100 V/ns.

TABLE I. MATERIAL PROPERTIES OF SI, GAN AND SIC [1]

Parameter	Unit	Si	GaN	SiC
Band Gap	eV	1.12	3.39	3.26
Critical Field	MV/cm	0.23	3.3	2.2
Thermal conductivity	W/cm·K	1.5	1.3	3.8
Electron Mobility	cm ² /V·s	1400	1500	950

The high switching frequency is an improvement in efficiency of power electronics but a challenge for EMC performance. The conducted electromagnetic interferences increases significantly with the use of WBG power devices. In [2] the conducted EMI emissions of motor drivers based on WBG are investigated. There it is shown, that emissions of a WBG device with used switching frequencies above 50 kHz are much higher. The small rise time create a wide frequency spectrum. Hence, the high frequencies cause serious coupling to other wires nearby.

III. COMMUNICATION NETWORKS

In this section, a brief description of the used communication networks LIN and CAN is given. It is focused on the bus properties, which are important for further investigations on electromagnetic compatibility.

A. Single wire communication network

The most commonly used single wire communication network in automobiles is the Local Interconnect Network (LIN), which is defined in ISO 17987. LIN was introduced as a low cost connection of mechatronic components (e.g. window lifter, wiper) with low data rates up to 20 kbit/s [5]. LIN is a single master system and uses an operating voltage of 12 V. The single wire is susceptible to interference. To face this problem, LIN uses a slow transmission rate and admits a high tolerance of the voltage level deviation of up to 40 % [6].

B. Twisted Wire Pairs Communication Network

The most commonly used cable in automotive communication networks is the twisted wire pair (TWP). Examples of TWP applications are CAN, FlexRay and Automotive Ethernet. A TWP consists of two identical wires, which are twisted together to improve electromagnetic compatibility. This transmission system evaluates the differential signal of two wires for logic levels. Therefore, differential mode interferences have the highest impact on signal integrity and are subject of the following investigations. Twisting the pairs counters the effect of interferences on each half twist to minimize the differential mode interferences at the end of the wire. [7].

As an exemplary bus application based on differential signaling, Controller Area Network (CAN) and CAN-FD (flexible data rate) is chosen. CAN and CAN FD are used to connect different electronic control units with complex cable structures. This multi-master serial bus uses a linear bus termination with 120 Ω and reaches data transmission rates up to 1 Mbit/s or up to 8 Mbit/s (CAN FD) [5]. The differential voltage range is 0 to 2 V with a dominant logic level of 2 V. CAN is standardized in ISO 11898 [8].

IV. MODELING

In the following section, the modeling approaches for the investigated configuration are presented. Simulations allow

the estimation of the interference voltages and the reliability of communication networks. The description of the model is divided into three parts: the coupled wires, the bus transceivers and finally the power electronic system.

A. Coupled Wires

In this section, the modeling approach for the coupled wires is described. The crosstalk of parallel wires can be described with basic equations of the transmission line theory. Assuming infinitesimal short wires oriented in z-direction, a lumped-circuit model can be used. One Δz section of the wires can be defined with $n \times n$ per-unit-length matrices (with n as number of wires) [9]. In the following sections lossless wires are considered ($R' = 0$ and $G' = 0$). The wire parameters C' and L' can be computed based on the geometry of the configuration. Assuming homogeneous surrounding media and larger distances between the wires, the parameters can be estimated with simple analytic formulas, e.g. [10]. Here, the simple approaches are applied, as only rough estimations should be given. In Fig. 2 the geometry of the considered parallel wires is depicted. The parameter d_{sc} determines the distance between the power electronic wire and the first communication wire (wire 2). In a setup with a single wire communication network, there are just wire 1 and 2. In a setup with three wires the distance between the two communication wires is defined as d_c . All examined wires have the same height $h = 0.05$ m above ideal ground and the same effective length of l . The radii of the used wires are $r_{2,3} = 0.334$ mm and $r_1 = 0.691$ mm based on utilized wires in the measurement setup (Section VI).

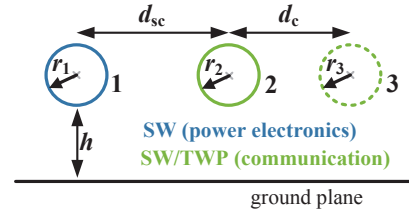


Fig. 2. Geometric configuration of parallel wires

Using the transmission line theory for multiconductor transmission lines, the current vector $I(z)$ and voltage vector $V(z)$ can be introduced. The resulting description are coupled linear differential equations (1) using the per unit length matrices Z' and Y' of the wire configuration. A detailed description can be found in [9].

$$\frac{d^2 \underline{V}(z)}{dz^2} - \underline{Z}' \underline{Y}' \underline{V}(z) = \mathbf{0} \quad (1a)$$

$$\frac{d^2 \underline{I}(z)}{dz^2} - \underline{Y}' \underline{Z}' \underline{I}(z) = \mathbf{0} \quad (1b)$$

These differential equations can be solved in frequency domain with the principal axis theorem to get voltage and current at both ends of wires depending on termination resistances. This approach is described in [11] and is implemented in Matlab. To obtain results in time domain Inverse Fast Fourier Transform (IFFT) is used. The usage of the parallel wire model for the TWP setup is described in detail in chapter VI.B. Besides, the two wire configuration is modeled with the circuit simulator ngspice and the ngspice model CPL. Due to convergence problems ngspice is not used for the three wire configuration simulation.

B. Bus Transceivers

For simulation of the bus systems, the essential parts must be modeled. Besides the wires, the bus transceivers' terminating impedances have to be modeled. At first, the model of the LIN Bus transceiver will be described. Assuming the nodes being in receiving mode, LIN nodes are simulated with an input impedance $R_{LIN} = 30 \text{ k}\Omega$ and $C_{LIN} = 220 \text{ pF}$ [6]. The model for the LIN Bus configuration is shown in Fig. 3. The interference voltage drop across the termination network ($v_i(t)$) is the disturbing signal on the bus system.

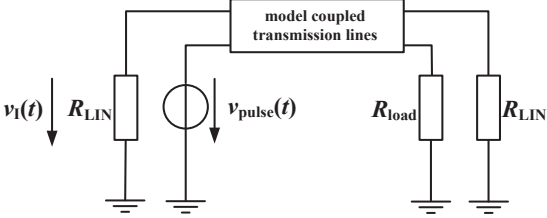


Fig. 3. Model: LIN Bus

CAN uses differential signaling between two wires. According to the ISO 11898 standard specification, the bus is terminated at both ends with the characteristic impedance 120Ω . Split termination is used to filter and stabilize the common mode of the bus. The concept is shown in Fig. 4. The elements are given with $R_{CAN} = 60 \Omega$ and $C_{CAN} = 4.7 \text{ nF}$.

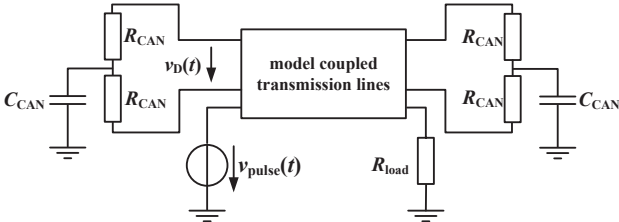


Fig. 4. Model: CAN Bus

C. Power Electronic System

The control device in the power electronic system is modeled as an ideal voltage source. The output signal is a rectangular pulse, which emulates a PWM signal created by WBG semiconductors in power electronics. The amplitude range of the pulse is from 0 to 48 V and the rise time is 3 ns. These parameters are chosen based on a GaN transistor evaluation board [14]. The repetition frequency is 100 kHz to emulate a common PWM signal. Besides, the load in the power electronic system is modeled as an ohmic load. The load impedance is $R_{load} = 1 \Omega$ to submit a high current and power flow. The circuit representation is shown in Fig. 3 and Fig. 4.

V. VALIDATION OF SIMULATION APPROACH

In the following section, measurement results are presented to validate the introduced modeling approach. The measurement setup is described and simulation results of reference setups are compared with measurement data.

A. Measurement Setup

To investigate the coupling of wires, a measurement setup has been applied. Parallel wires with the length of 1.8 m are arranged over a copper table with a constant height of 5 cm. To generate the needed pulses, a GaN E-HEMT half bridge evaluation board by GaN Systems is used [12]. The investigation with 48 V pulses required the use of the half bridge output

signal. The evaluation board is modified to implement the required output signal. The inductor of the board is removed to enable a direct connection to the output of the half bridge. The wire from the pulse generator is terminated with an ohmic load. The following investigations are executed with a constant frequency of 100 kHz, which is generated by an external signal generator. The single wire or twisted wire pairs are arranged in variable distances to the power electronic wire. The transmission lines of the communication system are terminated with the input impedances of LIN or CAN transceivers, as described in chapter V. The whole measurement setup is depicted in Fig. 5. In the upper part of this figure, the whole setup is shown. In the lower part, the GaN board and the wire configurations are depicted in detail. The wires are fixed to ensure a constant distance for reproducible measurements. The two and three wire configurations are also shown in this figure. Furthermore, the CAN wire loop assumed close to a connector can be seen.

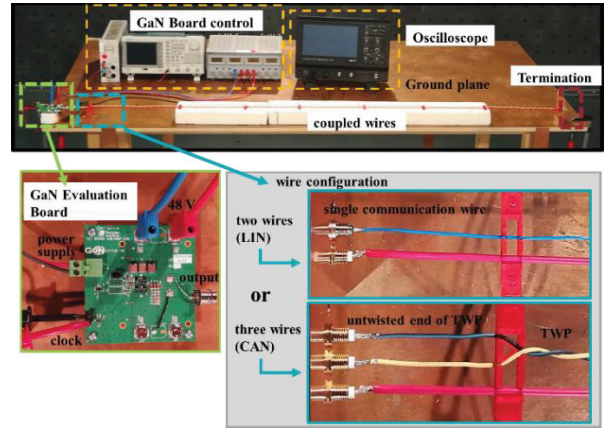


Fig. 5. Laboratory setup

B. Validation Results

In this section, simulations based on the presented model approaches to wires and bus transceivers are compared to measurement results. The general configuration has been described in the previous section. First, a two wire configuration is validated. The GaN board generates a pulse with fundamental frequency $f = 100 \text{ kHz}$ and a duty cycle of 35%. The wire is loaded with $R_{load} = 40 \Omega$ to limit the setup's power dissipation. The communication network is terminated with $30 \text{ k}\Omega$ as defined in LIN specification. The length of both wires is $l = 1.8 \text{ m}$ and the distance amounts $d_{sc} = 5 \text{ mm}$. In Fig. 6, simulation and measurement results of the near-end voltage on the receptor wire are shown. The model simulates the voltage waveform properly.

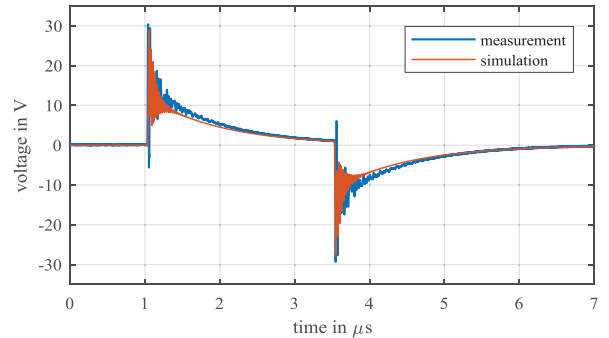


Fig. 6. Near-end voltage validation results for LIN Bus configuration ($d_{sc} = 5 \text{ mm}$, $l = 1.8 \text{ m}$)

The configuration with three parallel wires will be validated up next. The GaN Board with the following settings is used: $f = 100$ kHz and a duty cycle of 10 %. Hence, the differential signaling of the two wire communication networks, the differential voltage on the receptor wires is evaluated. The length of the parallel wires is $l = 1.8$ m and the distances are $d_{sc} = 5$ mm and $d_c = 10$ mm. The termination at both ends is 120Ω . The comparison of measurement and simulation results is shown in Fig. 7. The simulations deliver good results and allow simulative investigations besides parameter studies.

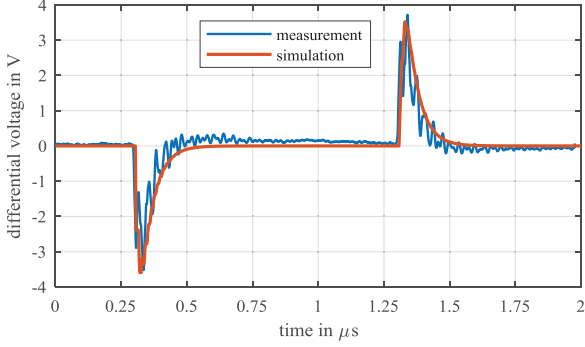


Fig. 7. Nearend differential mode voltage validation results for CAN Bus configuration ($d_{sc} = 5$ mm, $d_c = 10$ mm, $l = 1.8$ m)

VI. APPLICATION AND DISCUSSION

In this section, simulation results based on the validated model approaches are presented. The influence of different geometric parameters is analyzed and the impact on reliable data transmission by interference voltage is discussed.

A. Single wire communication network

The first investigation focuses on LIN bus communication. The model validated in section V is used to analyze the interference voltage in different geometric configurations. This investigation aims to find critical configurations for data transmission. The logic level of LIN is 12 V and the first assumption of a critical influence voltage is the reach of 12 V at peak. In Fig. 8 the simulation results of the interference voltage on the receptor wire at the near-end are shown. The blue curve shows the maximum interference voltage depending on the distance d_{sc} between the two wires. It can be seen, that the absolute maximum interference voltage decreases with an increasing distance between the wires. In case of the varying distance the length of the coupled wires is kept constant at $l = 0.05$ m. As a reference voltage the 12 V logic level of LIN is also illustrated. The value of the maximum interference voltage descends beneath 12 V at a distance of $d_{sc} = 17$ mm. These results show that the peak voltage on the receptor wire may reach critical values. The second waveform describes the interference voltage depending on the length of the coupled wires. The distance d_{sc} between the wires is 10 mm. It can be seen, that the interference voltage decreases with decreasing length l . At first, the voltage rises, with increasing coupling length the maximum interference voltage approximates a constant value of 22 V. This threshold value depends on the chosen distance d_{sc} between the wires.

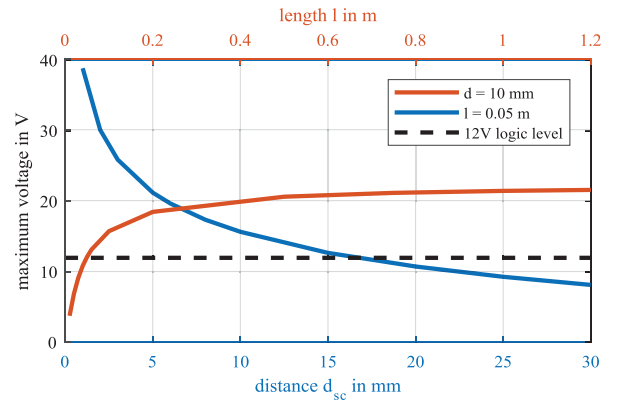


Fig. 8. Maximum voltage at near-end on the receptor wire depending on geometry parameters

The results show, that the absolute maximum voltage exceeds the logic level of 12 V. If the disturbing voltage rises above 12 V a bit shifting is generally possible. The duration of the interference voltage and its relation to the bit duration has a great influence on the reliable data transmission. Therefore, a condition of critical influences is defined to estimate a disturbance. The data transmission can be affected, if 30 % of bit duration T_{Bit} is affected by a disturbing signal that is high enough to cause a bit shift. The mathematical description of this consideration is depicted in (2). The variable V_T conforms the critical voltage level, which is needed to cause a bit shift. For investigated LIN bus the threshold voltage equates to 12 V. The period within the differential voltage has to exceed the threshold is defined by the bit duration of LIN $T_{Bit} = 50 \mu s$ ($f_{Bit} = 20$ kbit/s).

$$v(t) > V_T \quad \forall t \in [t_0, t_0 + 0.3 \cdot T_{Bit}] \quad (2)$$

To illustrate this condition, in Fig. 9 two simulation results of interference voltage are shown and compared with a LIN bit pulse. The distance between the coupled wires is defined with $d_{sc} = 5$ mm and the PWM pulse duration is $20 \mu s$. The simulation results of $l = 0.5$ m is a narrow peak which increase the logic level of 12 V. This interference voltage does not lead to a disturbance of LIN communication due to the introduced condition (2), because of the small pulse width. The duration of the interference voltage exceeds with coupled length. To meet the condition (2) a coupled wire length of 30 m is required. Such large coupling length can hardly be found in typical LIN applications and can be seen as non-critical.

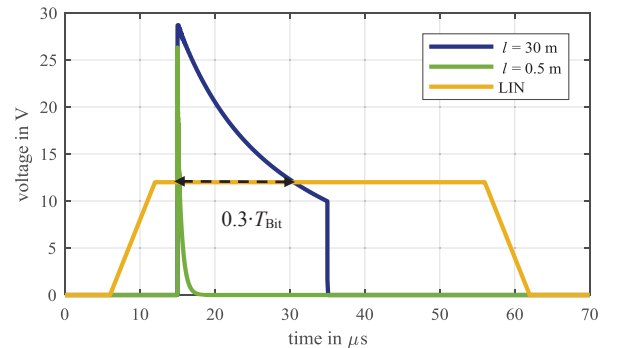


Fig. 9. Comparison of LIN bit pulse and simulation results ($d_{sc} = 5$ mm)

B. Twisted wire communication network

In this section, the model is utilized to estimate the potential risk on communication networks with differential signaling. Under real conditions, the wires have to be connected to pin connectors at the communication node. This technical premise leads to an untwisted part of the wire. This part with parallel wires builds up a loop, as illustrated in Fig. 10, which affords differential mode interferences. The assumption for the investigation is an ideal twisted pair and a parallel wire configuration at the wire connectors. The twisted part of the wire is assumed to be ideal and inductive coupling is compensated, i.e. the twisted part of the wire has no effect on the coupling and the disturbing voltage [13]. The untwisted part of the wire has a length of $l = 0.05$ m in the following investigations. The denotation of the distances between the wires has already been introduced in Fig. 2.

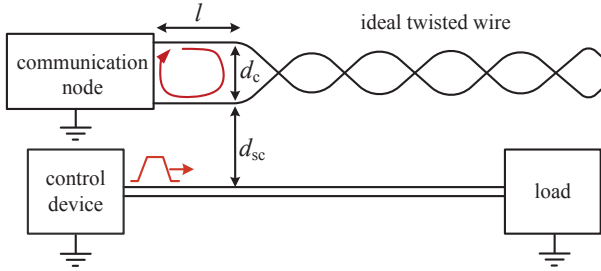


Fig. 10. Configuration with an untwisted end of the twisted wire

At first, the reached maximum differential voltage is analyzed. The distances d_{sc} and d_c are varied in different simulations. The exemplary results of two parameter variations are shown in Fig. 11. Each of the two x-axis varies one distance, while the other distance has the constant value of 5 mm. At first the influence of the varied distance d_{sc} is analyzed. The differential voltage on the receptor wires decreases with an increasing distance. This behavior results from the same effect as seen in the two wire configuration. On the other side, the increasing distance d_c leads to an increasing differential voltage. The wider distance of wire 3 to the generator wire leads to a more asymmetrical setting and the interference voltage on the wires differs more. Nearly every simulation shows a maximum voltage above the CAN logic level of 2 V. In CAN standard the dominant level is determined with a differential voltage level above 0.9 V and a recessive level is detected underneath 0.5 V [8].

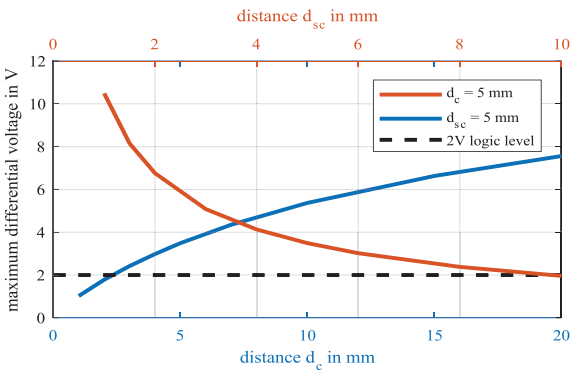


Fig. 11. Maximum differential voltage on a twisted wire pair with an untwisted cable end of $l = 0.05$ m

To estimate the immunity of active CAN FD communication concerning pulse disturbance, measurements were done.

Based on these measurements, influence of WBG semiconductors can be evaluated. The measurement setup consists of two CAN FD boards [13] and a point-to-point communication with data transmission rate of 6 Mbit/s is established. The boards are connected with a twisted pair wire and the transmitted data are just a continual alternation of dominant and recessive bits. The disturbance is synthesized by a signal generator and injected into one of the twisted pair wires. Hereby, a toroidal ferrite is used as an inductive transducer with primary and secondary windings of two turns each. The induced signal is superposed with the communication signal of one wire and leads to a differential mode disturbance. Within this setup the immunity of communication depending on the disturbance pulse parameter amplitude U_D and pulse width t_D is analyzed. An exemplary measurement result is shown in Fig. 12 (b). The disturbance is induced in the CAN-L wire and leads to a failure in the received signal. It has to be mentioned, that the time of occurrence of the disturbing pulse is an influencing factor of disturbing effects, causing by differential signaling. The evaluation results of these measurements are shown in Fig. 12 (a). In the figure amplitude U_D and pulse width t_D combinations are shown and if the created disturbing pulse leads to a failure of bit detection. The results are illustrated relatively to the maximum voltage change on one wire U_{CAN} and the bit duration T_{Bit} . Based on this measurement results the condition (2) can be parametrized. The threshold can be chosen as 1.5 V and the period, within the differential voltage has to exceed the threshold, is defined by 30 % of bit duration ($T_{Bit} = 170$ ns, $f_{Bit} = 6$ Mbit/s).

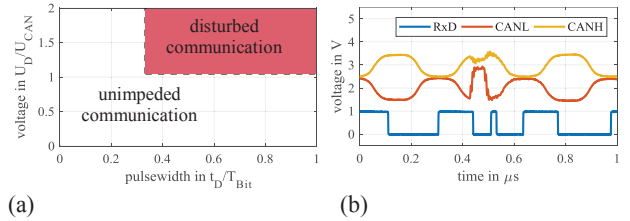


Fig. 12. (a) Measurement results of CAN FD communication immunity, (b) exemplary measurement results

Simulation results of exemplary differential voltage waveforms are shown in Fig. 13. The differential voltage is computed for two different geometric configuration and compared with a CAN FD bit pulse. The green curve reaches the value of 2 V just for a short period of time. This configuration can be seen as uncritical according to this simulation results. The blue curve exceeds the logic level for a duration greater than 30% of bit duration. This configuration can lead to a bit shift and the communication can be impeded.

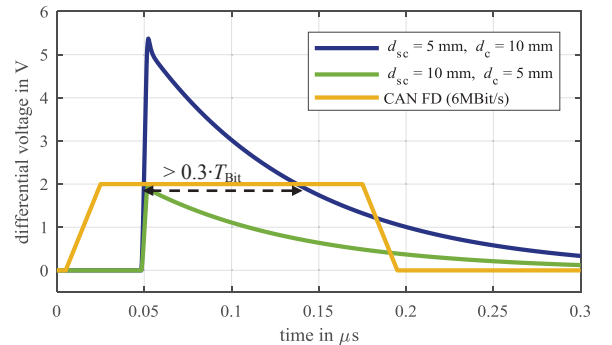


Fig. 13. Comparison of CAN FD bit pulse and simulation results ($l = 0.05$ m)

To find the critical geometric parameter configurations condition (2) is evaluated. The interference voltage is computed and estimated depending on the two geometric parameters d_c and d_{sc} (see Fig. 10). Different combinations of these parameters are analyzed and the results are shown in Fig. 14. In the colored area, the condition is met. For an untwisted wire length of $l = 0.05$ m, many configurations lead to critical differential voltages. Bit shifting is possible in the investigated configuration. The simulation results were validated with three measurement configurations. The measurements were made with the setup described in chapter V.A and the CAN FD boards [13] with a 6 Mbit/s transmission rate. Three geometric configurations were used and the results are also marked in the figure with crosses. The measurement results confirm the risk of disturbed communication.

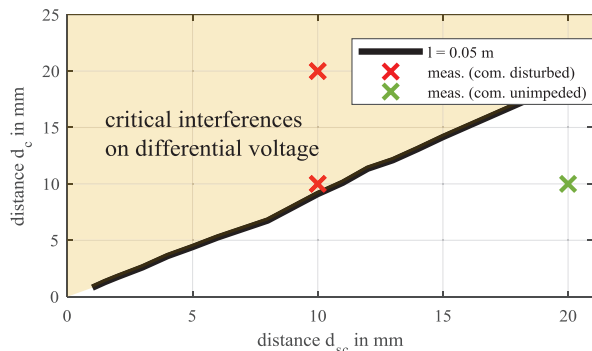


Fig. 14. Critical geometric parameters acc. Fig. 10 in three wire configuration for CAN FD communication

It can be seen, that the bit duration is an important factor, because the percentage of the disturbing signal varies depending on the bit duration T_{Bit} . In the worst case, the message of the communication network does not reach the recipient or incorrect data is received. The bus error handling will resend the message in case of a detected error, but hereby, the transmission time will be increased. According to the priority of the message, the functionality will be significantly impeded.

VII. CONCLUSION

This paper investigates the EMI coupling mechanism of a power electronic wire and communication transmission lines. A model approach for this configuration has been introduced and validated with measurement results. The simulation gives good results and has been used in further analyzes. The simulations have been used to evaluate influences of geometric parameters on disturbing signals. The peak voltage and the pulse

width of the interference voltage have been computed in LIN and CAN communication networks. The PWM signals, generated by WBG semiconductors with amplitude of 48 V, lead to significant disturbing signals in the communication networks. The configuration of an untwisted cable end of a twisted wire pairs even leads to differential mode interferences, which can disturb the data transfer. The negative effects on the communication quality decreases with higher transmission rate as used in automotive Ethernet or FlexRay. Therefore, further investigations on wire coupling and the impact on communication nodes have to be done to ensure a reliable performance in communication networks adjacent to WBG based power electronic networks.

REFERENCES

- [1] A. Lidow, *GaN Transistors for Efficient Power Conversion*, Chichester, Great Britain: Wiley, 2014
- [2] D. Han, S. Li et al., "Comparative Analysis on Conducted CM EMI Emission of Motor Drives: WBG Versus Si Devices," *IEEE Trans. Ind. Electron.*, vol. 64, no. 10, Oct 2017
- [3] H. Chen, T. Wang, "Estimation of Common-Mode Current Coupled to the Communication Cable in a Motor Drive System," *IEEE Trans. On electrom. comp.*, vol. 60, no. 6, 2018
- [4] K. S. Boutros, R. Chu and B. Hughes, "GaN Power Electronics for Automotive Applications," *IEEE Energytech*, 2012
- [5] K. Reif, *Automobilelektronik*, Wiesbaden, Germany: Vieweg&Sohn, 2007
- [6] ISO-17987, Road Vehicles-Local interconnect network (LIN), International Standards Organization, 2016
- [7] C. R. Paul, J. W. McKnight, "Prediction of Crosstalk Involving Twisted Pairs of Wires – Part I: A Transmission-Line Model for Twisted-Wire Pairs," *IEEE Trans. on electrom. compt.*, vol. 21, no. 2, 1979
- [8] ISO-11898, Road Vehicles - Controller area network (CAN), International Standards Organization, 2015
- [9] C. R. Paul, *Introduction to electromagnetic compatibility*, 2nd ed. Hoboken, NJ, USA: Wiley, 2006
- [10] F. M. Tesche, *EMC Analysis methods and computational models*, New York, USA: Wiley, 1997
- [11] C. R. Paul, *Analysis of multiconductor transmission lines*, Piscataway, NJ, USA: Wiley, 2008
- [12] *GS61008P-EVBHF GaN E-HEMT Half Bridge Evaluation Board – User's Guide*, Rev. 180227, GaN Systems, Canada, 2018
- [13] C.R. Paul, M. B. Jolly, *Sensitivity of Crosstalk in Twisted-Pair Circuits to Line Twist*, *IEEE Trans. on electrom. compt.*, vol. 24, no. 3, 1982
- [14] *User Manual DSO-8/TSON-8 Demoboard-Z8F62791012*, Rev. 1.0, infineon, 2018